An Evaluation of Nine ARW-WRF Microphysics Schemes for Solar Power Forecast in Arizona

Yang Cao, William Holmgren, Michael Leuthold, Eric Betterton, Christopher Castro, Antonio Lorenzo, and Hsin-I Chang

Department of Hydrology & Atmospheric Sciences The University of Arizona

Introduction

- Surface solar irradiance forecasts are largely influenced by cloud structure, dynamics, and radiative transfer that are modulated by cloud microphysical processes in the model.
- We studied 19 days with subjectively good initializations under deep convection, high, middle, and low cloud scenarios.
- We assessed the accuracy of the WRF irradiance forecasts by comparing them to irradiance derived from GOES visible and infrared channels, as well as a network of surface observations.
- We regridded the 1-km satellite-derived global horizontal irradiance (GHI) dataset (708 x 627 points) to a 1.8-km model mesh (420 x 354 points) using the inverse distance squared weighting method to enable quantitative analyses.
- Synthetic brightness temperature (Tb) imagery at 10.7 μm of simulated cloud fields was created from model runs using NCEP Unified Post Processor (UPP).

Cases studied

- Optically **thick** cloud scenarios ($\tau > 23$): 01 Mar 2014, 16 Nov 2015, 07 Jan 2016.
- Optically **medium** cloud scenarios (τ: 3.6-23):
  low-mid level (top>440mb): 03 Aug 2014, 05 Jan 2016, 04 Aug 2016, 08 Aug2016, 26 Aug 2015, 24 Aug 2015.
  high level (top<440mb): 08 Sep 2015, 18 Feb 2016, 09 Sep 2015, 28 Oct 2015, 18 Jan 2016, 05 Mar 2016.
- Optically **thin** cloud scenarios ($\tau < 3.6$): 11 Mar 2016, 23 Jan 2016, 23 Feb 2016, 29 Feb 2016.

Available observations

GOES-15 imagery-derived GHI images
- Horizontal grid spacing: **1 km**
- **708 x 627** points
- Algorithm: University of Arizona Surface Irradiance Based Satellite (UASIBS) (Kim et al. 2016)
- Derived from GOES-15 infrared and visible channel data
- See **Figure 2a** as a GHI map example.

Figure 3 shows its synthetic Tb imagery.

Surface GHI observations
- 7 APS stations and 1 UA site (see **Figure 1** inset)
- Sampling interval: 3-min instantaneous values
- Averaging interval: 1 hour

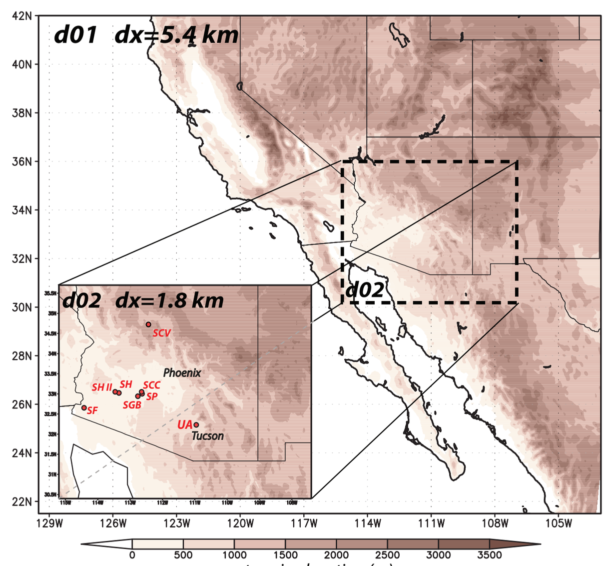

Figure 1
Domain configuration for the ARW simulations, with topography shaded. Domains 1-2 employ horizontal grid spacings of 5.4 and 1.8 km, respectively. The inset shows an enlarged version of domain 2, with surface irradiance observation locations (red dots) marked.

WRF-ARW configuration

Table 1. Model setup.

Model Settings	WRF v3.7	
Domain	D1	D2
Horizontal grid spacing [km]	5.4	1.8
Num of horizontal mesh	460 x 440	420 x 354
Num of vertical layers	38 (model top: 100 hPa)	
Microphysics	vary (see Table 2)	
Longwave radiation	RRTMG	
Shortwave radiation	RRTMG	
Land surface	Noah	
Surface layer	Pleim-Xiu	
Planetary boundary layer	ACM2 / YSU / BouLac *	
Cumulus convection	off	
Landuse database	updated USGS	
Initialization	NAM 12km grids, 1200 UTC cycle	
Boundary conditions	one-way nesting	
Output interval	3 min	

Table 2. Microphysics schemes adopted.

Microphysics Scheme	References	Mass Variable	Number Variable
Goddard (GODD)	Tao et al. (1989)	Qc Qr Qi Qs Qg	N/A
Milbrant-Yau (MILB)	Milbrandt and Yau (2005)	Qc Qr Qi Qs Qg Qh	Nc Nr Ni Ns Ng Nh
Morrison (MORR)	Morrison et al. (2009)	Qc Qr Qi Qs Qg	Nr Ni Ns Ng
CAM5.1 (CESM)	Neale et al. (2012)	Qc Qr Qi Qs Qg	Nr Ni Ns Ng
SBU-YLIN (SBUY)	Lin and Colle (2011)	Qc Qr Qi Qs	N/A
WDM5	Lim and Hong (2010)	Qc Qr Qi Qs	Nn Nc Nr
WDM6	Lim and Hong (2010)	Qc Qr Qi Qs Qg	Nn Nc Nr
Thompson (THOM)	Thompson et al. (2008, 2009)	Qc Qr Qi Qs Qg	Ni Nr
Thompson aerosol-aware (THOM-A)**	Thompson and Eidhammer (2014)	Qc Qr Qi Qs Qg	Ni Nr Nwf Nif

* PBL treatments exerted only secondary influences on the model forecast skill for this study.
** An auxiliary aerosol climatology (year 2001-2007) file was placed into WRF through the WPS program.

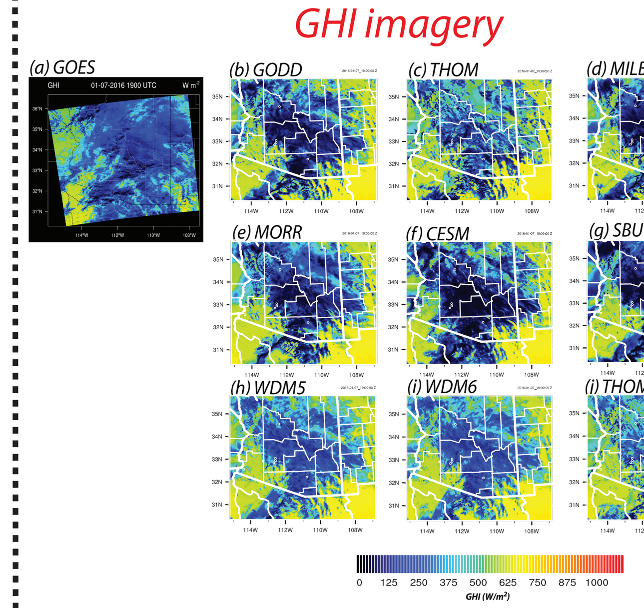

Figure 2
Surface GHI (W/m^2) for (a) GOES, (b) GODD, (c) THOM, (d) MILB, (e) MORR, (f) CESM, (g) SBUY, (h) WDM5, (i) WDM6, and (j) THOM-A, valid at 1900 UTC 07 Jan2016.

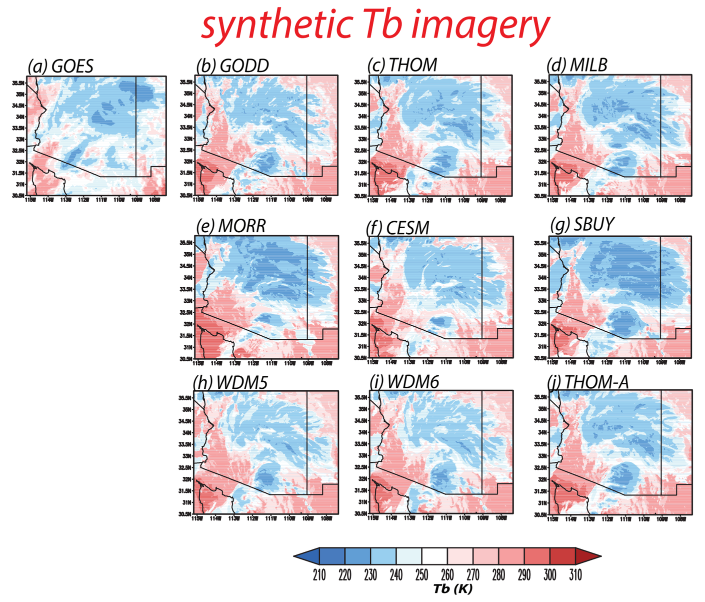

Figure 3
Cloud top brightness temperature (K) for (a) GOES, (b) GODD, (c) THOM, (d) MILB, (e) MORR, (f) CESM, (g) SBUY, (h) WDM5, (i) WDM6, and (j) THOM-A, valid at 1900 UTC 07 Jan2016.

Validation metrics

- For each forecast snapshot, the UASIBS-generated 1-km GHI imageries and model-generated 1.8-km GHI ("swdown") imageries were regridded onto a common 1.8-km horizontal grid spacing grid mesh.
- Verification time frames were defined as a time period when all satellite and model output GHI images have valid non-zero data coverage.
- Critical success index (CSI), mean absolute error (MAE), and mean bias error (MBE) were employed for satellite pixel-based validation and surface site-based validation.

$$\mathrm{CSI} = \frac{A}{A+B+C}$$

*A is correct yes forecasts of an event of cloudiness (defined as when pixel-based GHI falls below 90% of the clear sky GHI), B is false alarm forecasts, and C is misses. CSI range: **0** (no skill) - 1(perfect skill).*

$$\mathrm{MAE} = \frac{1}{n}\sum_{i=1,j=1}^{n}\left|GHI_{WRFi,j} - GHI_{obsi,j}\right|$$

$$\mathrm{MBE} = \frac{1}{n}\sum_{i=1,j=1}^{n}\left(GHI_{WRFi,j} - GHI_{obsi,j}\right)$$

i: model pixel or site, j: time frame; n~ 3,270,960 for satellite-based validation; n~2328 for 3min-interval surface pyranometer-based validation.

Table 3. Model Critical Success Index (CSI, unit: %) calculated based on GOES 15 imagery - derived GHI. (warm color: CSI score higher than MP ensemble average; cold color: CSI score lower than average; red: highest score for each case)

case		CT (mb)	COD	GODD	MILB	MORR	CESM	SBUY	WDM5	WDM6	THOM	THOM-A
optically thick	2014/3/1	332	26.1	69	68	68	79	72	69	69	67	63
	2015/11/16	567	25.2	54	57	54	58	57	55	54	52	50
	2016/1/7	436	23.7	74	76	75	79	79	74	73	71	67
	average	445	25.0	66	67	66	72	69	66	65	63	60
optically medium (low/mid level)	2014/8/3	470	14.4	75	77	73	83	75	77	76	74	73
	2016/1/5	603	12.5	73	74	74	84	71	79	78	75	65
	2016/8/4	470	11.9	36	38	35	42	42	36	36	34	34
	2016/8/8	505	11.7	27	28	29	31	30	29	25	24	22
	2015/8/26	453	10.3	39	38	38	41	39	37	38	35	33
	2015/8/24	458	6.8	31	32	32	31	34	30	28	31	29
	average	493	11.3	47	48	47	52	49	48	47	46	43
optically medium (high level)	2015/9/8	359	9.8	36	34	33	38	44	41	40	24	19
	2016/2/18	373	9.4	47	52	50	50	56	56	54	33	31
	2015/9/9	346	7.7	63	64	63	66	66	66	66	49	41
	2015/10/28	359	5.1	59	61	63	63	66	66	65	42	36
	2016/1/18	350	5.0	44	53	65	45	60	49	49	43	38
	2016/3/5	400	4.9	34	32	39	40	40	48	49	23	20
	average	365	7.0	47	49	52	50	55	54	54	36	31
optically thin	2016/3/11	344	3.6	58	60	72	41	70	56	54	43	34
	2016/1/23	357	2.9	64	67	75	52	74	63	63	59	51
	2016/2/23	610	2.7	19	17	26	18	21	13	17	15	16
	2016/2/29	526	2.5	17	14	24	9	21	15	15	14	4
	average	459	2.9	40	40	49	30	47	37	37	33	26
average of all cases		438	10.3	48	50	52	50	54	50	50	43	38

Results

- CESM scheme performed well at forecasting deep convection and low-mid level cloud cover (CSI, **Table 3**), yet generally overpredicted cloud optical depth(**Table 4**).
- Brightness temperature (Tb) PDFs show CESM substantially overpredicted middle and low clouds (240-285 K) when it exhibited a large negative bias (**Figure 4, Table 4**).

Table 4. Model mean bias error (MBE, unit: W/m^2) calculated based on GOES 15 imagery - derived GHI. (warm color: bias error smaller than MP ensemble average; cold color: bias error larger than average)

case		CT (mb)	COD	GODD	MILB	MORR	CESM	SBUY	WDM5	WDM6	THOM	THOM-A
optically thick	2014/3/1	332	26.1	-48	-54	-53	-104	-89	-4	-6	11	47
	2015/11/16	567	25.2	48	30	45	27	36	66	66	47	65
	2016/1/7	436	23.7	19	3	22	-15	-20	50	52	62	92
	average	445	25.0	6	-7	5	-31	-24	37	38	40	68
optically medium (low/mid level)	2014/8/3	470	14.4	43	45	108	-41	53	94	87	82	157
	2016/1/5	603	12.5	22	10	5	-63	23	30	31	1	50
	2016/8/4	470	11.9	-19	-32	-16	-108	-54	-2	-6	0	19
	2016/8/8	505	11.7	18	19	27	11	4	25	34	32	39
	2015/8/26	453	10.3	-18	-20	-16	-86	-26	-16	-16	-11	12
	2015/8/24	458	6.8	-42	-47	-44	-106	-69	-39	-37	-30	-9
	average	493	11.3	1	-4	11	-66	-12	16	15	13	46
optically medium (high level)	2015/9/8	359	9.8	67	75	85	71	45	63	69	109	120
	2016/2/18	373	9.4	66	51	67	62	41	48	52	100	107
	2015/9/9	346	7.7	-3	-10	-6	-80	-22	-8	-8	33	90
	2015/10/28	359	5.1	17	22	10	23	-16	-14	-12	72	78
	2016/1/18	350	5.0	67	52	10	73	22	60	60	75	82
	2016/3/5	400	4.9	45	54	25	49	4	13	4	77	82
	average	365	7.0	43	41	32	33	12	27	28	78	93
optically thin	2016/3/11	344	3.6	47	50	-12	85	-14	55	55	85	94
	2016/1/23	357	2.9	13	9	-46	50	-55	17	17	45	57
	2016/2/23	610	2.7	36	33	26	34	32	40	37	36	40
	2016/2/29	526	2.5	18	22	0	26	8	16	16	24	29
	average	459	2.9	28	29	-8	49	-7	32	31	48	55
average of all cases		438	10.3	21	17	12	-4	-4	25	25	44	65

- THOM-A and THOM schemes tended to underpredict clouds at all circumstances (**Table 4, Figures 4, 5**).
- SBUY and MORR had close-to-zero event-averaged biases for thin cloud scenarios (**Figure 5, Table 4**), however, close inspection of the brightness temperature PDF indicates the two schemes produced excessive amount of ice at the cold end (< 240 K) of the temperature spectrum (**Figure 4**).

TOA brightness temperature

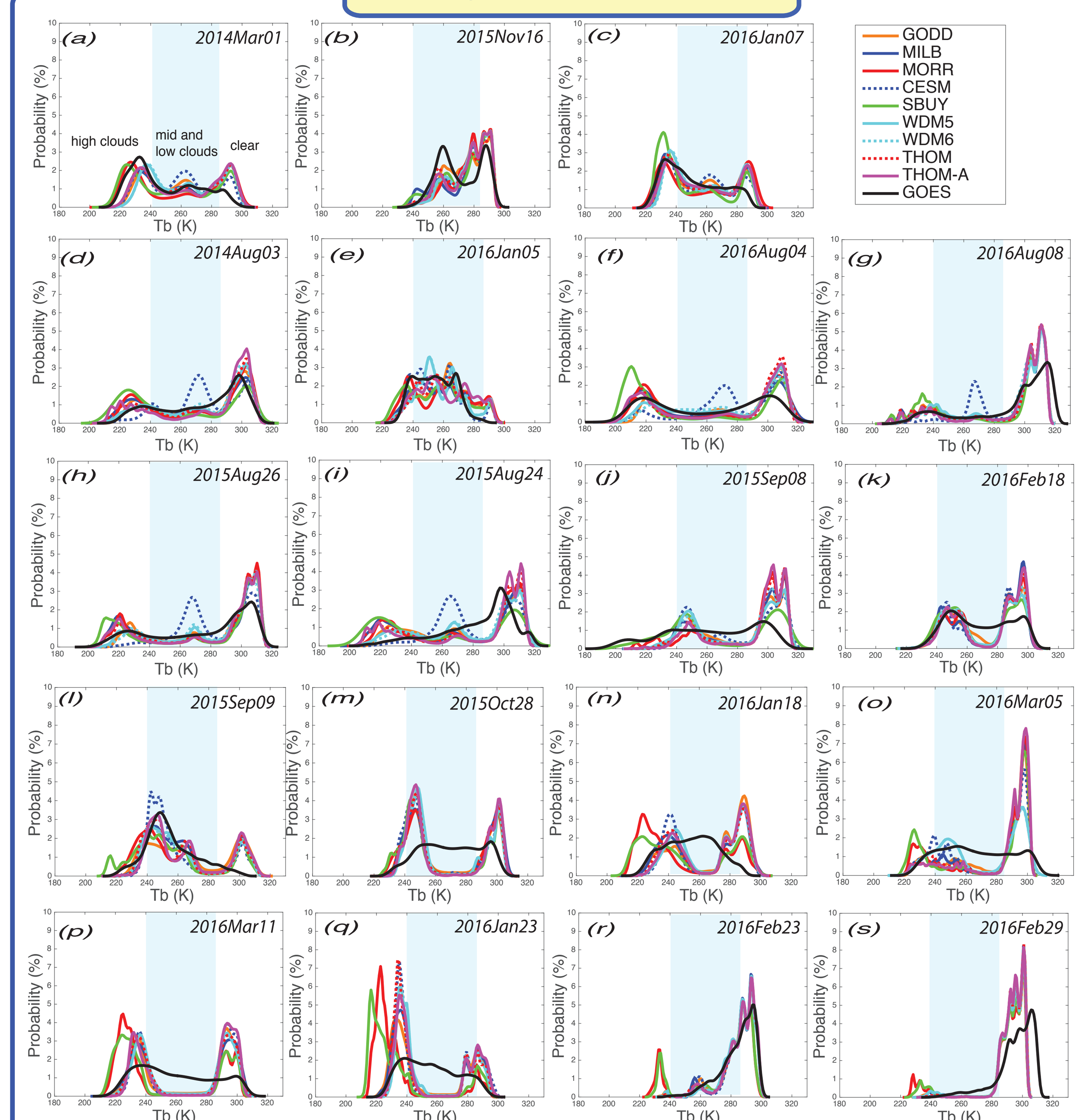

Figure 4
Probability of occurrence histograms for observed GOES-15 brightness temperatures (K) and synthetic brightness temperatures (K) simulated by model runs using GODD, MILB, MORR, CESM, SBUY, WDM5, WDM6, THOM, and THOM-A microphysical parameterizations, valid at 2300 UTC (11-hour forecasts).

- The verification results using the eight surface observation sites mostly resembled those using the satellite verification (**Figure 5**).
- For the thick cloud scenario, CESM and SBUY schemes had positive biases for the surface network verification.
- It is observed that most of the time, deep convection for the selected thick cloud cases mostly resided in the mountainous areas, so only a limited number of surface sites were affected by the thick cloud conditions and hence the three million pixel-based satellite verification should be more reliable.

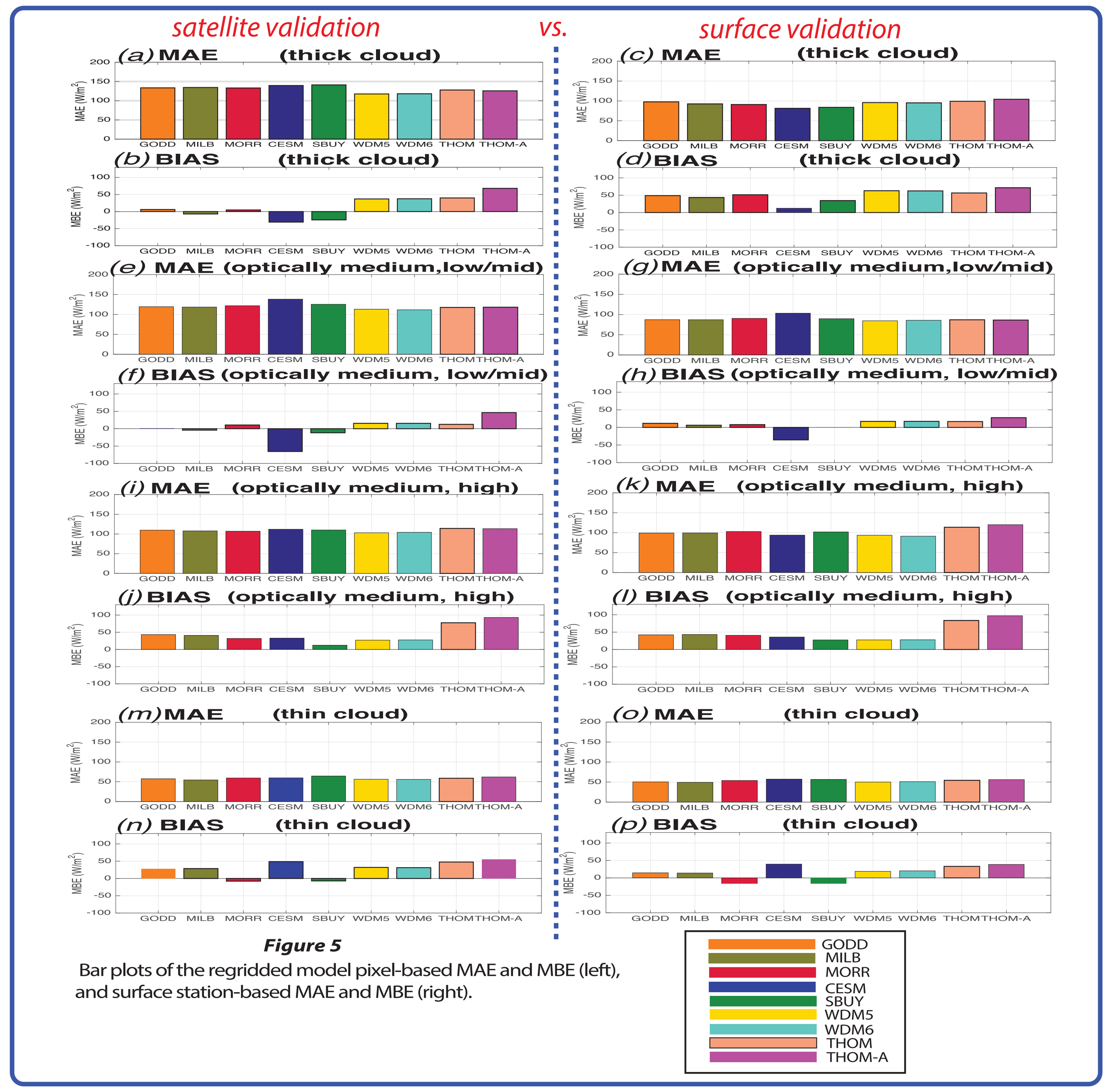

Figure 5
Bar plots of the regridded model pixel-based MAE and MBE (left), and surface station-based MAE and MBE (right).

Summary

- A uniquely superior bulk microphysics scheme does not exist for solar forecasting in Arizona.
- Most parameterizations tended to overpredict GHI for all cloud scenarios.
- MORR and SBUY had smaller biases for middle and high cloud scenarios.
- CESM scheme outperformed others at forecasting deep convection and low-level cloud cover, yet tended to overpredict cloud optical thickness.
- THOM and THOM-A schemes tended to underforecast cloud amount, especially for high clouds.
- THOM-A was found to dramatically overestimate cloud liquid-ice ratio (not shown).
- Synthetic satellite imagery showed usefulness in helping evaluate and understand microphysical parameterizations.

Contact information:
Yang Cao (sunnyyangcao@email.arizona.edu).

Acknowledgments: We would like to thank James Moker for helping with the regridding scripts. We also appreciate the advice from Professors Robert Fovell, Xubin Zeng, Xiquan Dong and Baike Xi. This work was supported by Tucson Electric Power and Arizona Public Service.